Latin American Journal of Solids and Structures
www.lajss.org

Sensitivity analysis of bridge-track-train system to parameters of railway

Abstract

Generally, Railway bridges are long structures which have different responses against different loads of train. Applied loads of train on railroad bridges are different in terms of axle loads speed, and annual passed tonnages and they have quite different dynamic behavior in comparison with road bridges. Most researches are basically focused on the quasi-static analysis. Therefore in these researches, the effect of load speed has been neglected. Nowadays with the development of rail transport systems, the study of dynamic behavior of bridges under the different load speed is necessary.

Also, the dynamic behavior of curved bridges is different than straight ones. In this paper, vertical and torsional vibrations of a curved beam have been studied with considering vertical, horizontal load and eccentricity of load than centerline of bridge. Also the considered parameters in this research are radius of curvature, track irregularity, vehicle speed and bridge span.

Keywords

horizontal curved bridges, freight train, dynamic analysis, dynamic bridge-train interaction

Jabar Ali Zakeri 1[a]
Morad Shadfar 2[b]
Mohammad Mehdi Feizi 3[c]

[a]Associate Professor, Iran University of science and technology, Hengam Street, Resalat Sq., Narmak, Tehran, Iran;zakeri@iust.ac.ir

[b]Research assistant, Iran University of science and technology, Hengam Street, Resalat Sq., Narmak, Tehran, Iran;morad_shadfar@rail.iust.ac.ir

[c]Research assistant, Iran University of science and technology, Hengam Street, Resalat Sq., Narmak, Tehran, Iran;mm_feizi@rail.iust.ac.ir

1 INTRODUCTION

Loads of trains on railroad bridges are different in terms of axle loads speed, and annual passed tonnages and they have quite different dynamic behavior in comparison with road bridges (Frýba, 1996)). In this regard, dynamic effects of moving vehicle in the most Regulations based on the impact factor (IF) and estimation of IF with static considerations. So in the most researches, the effect of vehicle speed is neglected (Yang et al., 2004). This mater was problem when it had been shown that the deflection of the bridge due to moving load and consequently stresses of the bridges were high in comparison with static ones significantly (Esmailzadehand Jalili, 2003). In addition, when vehicle moves on the bridge with critical speed, the bridge tends to have much deflection like the case the vehicle has a bigger axle load (resonance phenomena) (Yau, 2009).

With the development of high-speed railway system, the study of bridge dynamic due to different speeds of train is necessary. in addition with using materials which have high resistance the mass of the bridges reduce, consequently the bridges are more flexible (EsmailzadehandJalili, 2003) and also It causes particular problems especially in short span bridges. As an example in Lion-Paris the short span bridges show these defects (Zacher):

1. Crack and failure in concrete

2. Increasing the rate of ballast degradation due to high acceleration
3. Great distortions in track

Dynamic behavior of a railway bridge due to a passing train naturally is complicated and nonlinear phenomenon because the dynamic responses of a bridge due to a moving load is a function of train-bridge interaction and train parts in every time (Song et al., 2003). The problem of a beam subjected to a moving load was considered by Stokes and Willis (Zadeh 2010). Also Timoshenko presented a classic solution in 1922 for a beam subjected to a moving load with neglecting the inertia of the vehicle (Esmailzadeh andJalili, 2003;Zadeh, 2010). Jeffcott added the vehicle inertia in 1929 (Zadeh, 2010). Sadiku and Leipholz(Esmailzadehand Jalili, 2003)in 1987 compared the moving load, moving mass and equivalent moving load results and showed that the effect of inertia could not be neglected even though the vehicle has a little mass. Of course it must be mentioned that their results were for a specific mass and a specific velocity. It is also necessary that the works ofFryba(Fryba, 1972, 1976, 1980)in this field is pointed out. Fryba (1972) studied the effects of constant speed and constant damping in beam responses.

However in first the most of the researches are focused on straight bridges while there are few works for curved ones. Yang and Wu (2001) presented the analytical solution of a curved beam under vertical and radial loads, but even he didn't consider the effects of eccentricity for this case.

The innovation in this paper is the examination of vertical and torsional vibration of a curved beam with the consideration of vertical, horizontal loads and eccentricity of the loads to centerline of bridge. While no one has not investigated the effect of moving suspended mass over curved bridge with realistic operational parameters and only series of moving loads are interested for this type of bridge (this solution is valid for long span bridge Fryba (1972)).

2 MODELING OF THE BRIDGE-TRACK-TRAIN SYSTEM

When a train passes over a bridge, there are three separated parts. The first two parts are train and bridge, but the third part which determines the dynamic forces that are exerted to bridge structure and vehicle dynamics is coupling element or modeling the vehicle-bridge interaction. The importance of this matter is this part determines the bridge and vehicle responses. (Xia et al, 2007) In this study for determining the contact forces, the three dimensional linear theory of Kalker has been used. This theory presents the interacting effect of the vehicle with the track and curved beam. It will be expressed in detail in appendix. Equations of motion for different parts are gathered separately and with the help of coupling elements are attached in order to build a unite 3D coupled system. Appendix is added at the end of the paper.

3 THE VEHICLE MODEL

In this paper, hopper car with the capacity of $65m^3$ has been studied. This wagon is equipped with the Y25 freight bogies.

For simplicity and avoiding non-linear part in vehicle equations, the side bearers are replaced with viscous dampers. For this purpose with the help of hysteresis graphs of the side bearers and extracting the energy loss per cycle, the equivalent viscous damping has been obtained. The mathematical model of the vehicle is shown in Fig. 1.

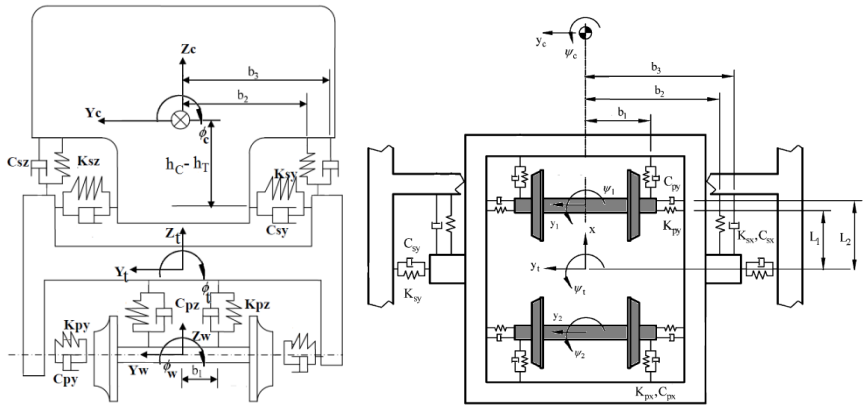

Figure 1: Mathematical model of the vehicle

3.1 The wheelset equations

In order to modeling wheel/rail contact forces (with consideration of lateral displacement and yaw rotation), the linear creep model has been used. For this purpose, it is only enough to set saturation coefficient (α) equal to 1 in non-linear theory. This simplification gives reasonable accuracy in large radius curves. In the presented equations ψ, φ, ϑ, z and y denote yaw, roll, pitch, vertical and lateral degrees of freedoms respectively that have been shown in Fig. 2. The subscript of w, t and c indicate wheel, bogie and car body respectively (Iwnicki, 2003).

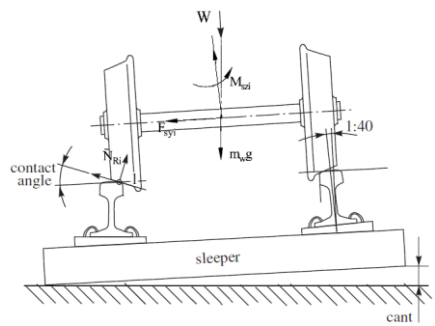

Figure 2: Freebody diagram of wheelset

$$
\begin{aligned}
& m_w\left(\ddot{y}_{wij}-\frac{V^2}{R}\right) \\
& =\frac{2f_{11}}{V}\left(\dot{y}_{wij}-V\psi_{wij}\right)-\frac{2f_{12}}{V}\left(\dot{\psi}_{wij}-\frac{V}{R}\right)-\frac{2r_0f_{11}}{V}\left(\frac{\lambda}{a}\right)\dot{y}_{wij} \\
& -\left(W_{ext}+m_w g+\frac{V^2W_{ext}}{gR}\phi_{se}\right)\left(\frac{\lambda}{a}\right)y_{wij}-\left(W_{ext}+m_w g\right)\phi_{se} \\
& +\frac{V^2W_{ext}}{gR}-2K_{py}y_{wij}-(-1)^j 2K_{py}L_1\psi_{ti}+2K_{py}y_{ti}-2C_{py}\dot{y}_{wij} \\
& -(-1)^j 2C_{py}L_2\dot{\psi}_{ti}+2C_{py}\dot{y}_{ti}+2K_{py}h_T\phi_{ti}+2C_{py}h_T\dot{\phi}_{ti}
\end{aligned}
\tag{1}
$$

$$
\begin{aligned}
&I_{wz}\ddot{\psi}_{wij} = -\frac{2a\lambda f_{33}}{r_0}y_{wij} + \frac{2f_{12}}{V}\dot{y}_{wij} - \left(I_{wy}\frac{V}{r_0} - \frac{2r_0 f_{12}}{V}\right)\left(\frac{\lambda}{a}\right)y_{wij} - 2f_{12}\psi_{wij} \\
&+\left(W_{ext} + m_w g + \frac{V^2 W_{ext}}{gR}\phi_{se}\right)a\lambda\psi_{wij} + 2K_{px}b_1^2\psi_{ti} + 2C_{px}b_1^2\dot{\psi}_{ti} \\
&-2K_{px}b_1^2\psi_{wij} - 2C_{px}b_1^2\dot{\psi}_{wij} - \left(\frac{2a^2 f_{33}}{V} + \frac{2f_{22}}{V}\right)\dot{\psi}_{wij} \\
&+\frac{2}{R}\left(a^2 f_{33} + f_{22}\right)
\end{aligned} \tag{2}
$$

$$
\delta_L = \delta_R = \lambda, \quad \frac{1}{2}\left(r_L - r_R\right) = \lambda y_{wij}, \quad \frac{1}{2}\left(r_L - r_R\right) = r_0 \tag{3}
$$

In this modeling, it has been assumed that when vehicles pass the curve, there is no flange contact between wheel and rail. This means that train is in vertical static position and vertical forces stay constant if there is no irregularity. For this reason, the wheels are modeled by conical wheels.

With this assumption the vertical forces can be calculated by eq. 4. It should be noted that the Kalker creep coefficients are variable by change in vertical force and wheel curvature but these coefficients are constant in conical wheel.

$$
N^{\,n}_{Lyij} = N^{\,n}_{Rzij} = \frac{1}{2}\left(W_{ext} + m_w g + \frac{V^2 W_{ext}}{gR}\phi_{se}\right) \tag{4}
$$

3.2 Bogie equations

There is no need to model bogie center bowl and its friction if the track radius is higher than 700m. Each bogie has 4 degrees of freedoms which contain two translational degrees (lateral and vertical) and two rotational degrees (roll and yaw) (Chenget al., 2009).

$$
\begin{aligned}
&m_t\ddot{y}_{ti} = -2K_{py}y_{wij} + 2C_{px}\dot{y}_{wij} + \left(-4K_{py} - 2K_{Sy}\right)y_{ti} + (4C_{py} - 2C_{sy})\dot{y}_{ti} \\
&+2K_{sy}L_c\psi_c + 2C_{sy}L_c\dot{\psi}_c + 2K_{sy}y_c + 2C_{sy}\dot{y}_c + 2K_{sy}\left(h_c - h_T\right)\phi_c \\
&+2C_{sy}\left(h_c - h_T\right)\dot{\phi}_c - 4K_{py}h_T\phi_{ti} - 4C_{py}h_T\dot{\phi}_{ti} + \left(\frac{V^2}{gR} - \phi_{se}\right)m_t g
\end{aligned} \tag{5}
$$

$$
m_t\ddot{z}_{ti} = 2K_{sz}z_c + 2C_{sz}\dot{z}_c - 2\left(K_{sz} + 2K_{pz}\right)z_{ti} - 2(C_{sz} + 2C_{pz})\dot{z}_{ti} + \left(1 + \frac{V^2}{gR}\phi_{se}\right)m_t g \tag{6}
$$

$$
\begin{aligned}
&I_{tx}\ddot{\phi}_{ti} = 2K_{sz}b_2^2\phi_c + 2C_{sz}b_3^2\phi_c - 2K_{sz}b_2^2\phi_{ti} - 2C_{sz}b_3^2\dot{\phi}_{ti} + [2K_{py}h_T + 4K_{pz}b_1^2\left(\frac{\lambda}{a}\right)]y_{wij} \\
&-4K_{py}h_T y_{ti} + \left[2C_{py}h_T + 2C_{pz}b_1^2\left(\frac{\lambda}{a}\right)\right]\dot{y}_{wij}
\end{aligned} \tag{7}
$$

$$
\begin{aligned}
&-4C_{py}h_T\dot{y}_{ti} - 2K_{py}h_T^2\phi_{ti} - 4C_{py}h_T^2\dot{\phi}_{ti} - 44K_{pz}b_1^2\phi_{ti} - 4C_{pz}b_1^2\dot{\phi}_{ti} \\
&I_{tz}\ddot{\psi}_{ti} = (-4K_{py}L_1^2 - K_{px}b_1^2 - 2K_{sx}b_2^2)\psi_{ti} + (-4C_{py}L_2^2 - 4C_{px}b_1^2 - 2C_{sx}b_3^2)\dot{\psi}_{ti} \\
&+2K_{py}L_1 y_{wi1} + 2C_{py}L_2\dot{y}_{wiL} + 2K_{px}b_1^2\psi_{wi1} + 2C_{px}b_1^2\dot{\psi}_{wi1} \\
&-2K_{py}L_1 y_{wi2} - 2C_{py}L_2\dot{y}_{wiL} + 2K_{px}b_1^2\psi_{wi2} + 2C_{px}b_1^2\dot{\psi}_{wi2} \\
&+2K_{sx}b_2^2\psi_c + 2C_{sx}b_3^2\dot{\psi}_c
\end{aligned} \tag{8}
$$

3.3 Car body equations

In the modeling of the Hooper wagon, degrees of freedom including lateral, vertical, roll, pitch and yaw has been opted. Equations 9-13 describe the dynamic behavior of car body (Cheng et al., 2009).

$$m_c\ddot{y}_c = -2K_{sy}\left(2y_c - y_{t1} - y_{t2}\right) - 4K_{sy}\left(h_c - h_T\right)\phi_c - 2C_{sy}\left(2\dot{y}_c - \dot{y}_{t1} - \dot{y}_{t2}\right) \\ -4C_{sy}\left(h_c - h_T\right)\dot{\phi}_c + \left(\frac{V^2}{gR} - \phi_{se}\right)m_c g \tag{9}$$

$$m_c\ddot{z}_c = -4K_{sz}z_c - 4C_{sz}\dot{z}_c + 2K_{sz}z_{t1} + 2C_{sz}\dot{z}_{t1} + 2K_{sz}z_{t2} + 2C_{sz}\dot{z}_{t2} + \left(1 + \frac{V^2}{gR}\phi_{se}\right)m_c g \tag{10}$$

$$I_{cx}\ddot{\phi}_c = 2K_{sz}b_2^2\phi_{t1} + 2C_{sz}b_3^2\dot{\phi}_{t1} + 2K_{sz}b_2^2\phi_{t2} + 2C_{sz}b_3^2\dot{\phi}_{t2} - 4K_{sz}b_2^2\phi_c \\ -2C_{sz}b_3^2\dot{\phi}_c - 4K_{sy}\left(h_c - h_T\right)y_c - 4C_{sy}\left(h_c - h_T\right)\dot{y}_c \\ +2K_{sy}\left(h_c - h_T\right)y_{t1} + 2C_{sy}\left(h_c - h_T\right)\dot{y}_{t1} + 2K_{sy}\left(h_c - h_T\right)y_{t2} \\ +2C_{sy}\left(h_c - h_T\right)\dot{y}_{t2} - 4K_{sy}\left(h_c - h_T\right)^2\phi_c - 4C_{sy}\left(h_c - h_T\right)^2\dot{\phi}_c \\ -4K_{sy}\left(h_c - h_T\right)L_c\psi_c - 4C_{sy}\left(h_c - h_T\right)L_c\dot{\psi}_c \tag{11}$$

$$I_{cy}\ddot{\theta}_c = -2K_{sz}z_{t1} + 2K_{sz}z_{t2} - 4K_{sz}\theta_c L_c - 2C_{sz}\dot{z}_{t1} + 2C_{sz}\dot{z}_{t2} - 4C_{sz}\dot{\theta}_c L_c \tag{12}$$

$$I_{cz}\ddot{\psi}_c = -4K_{sy}\psi_c L_c^2 - 4C_{sy}\dot{\psi}_c L_c^2 - 2K_{sx}b_2^2\left(2\psi_c - \psi_{t1} - \psi_{t2}\right) \\ -2C_{sx}b_3^2\left(2\dot{\psi}_c - \dot{\psi}_{t1} - \dot{\psi}_{t2}\right) - 2K_{sy}L_c\left(-y_{t1} - y_{t2}\right) \\ -2C_{sy}L_c\left(-\dot{y}_{t1} - \dot{y}_{t2}\right) \tag{13}$$

4 BRIDGE MODELING

The Common models of bridges include a simply supported beam that is subjected to a single moving load. These models are generally derived from works done by Timoshenko and Fryba (Esmailzadeh and Jalili, 2003).

Fig. 3 shows a beam with radius R that it illustrates general curved bridge model.

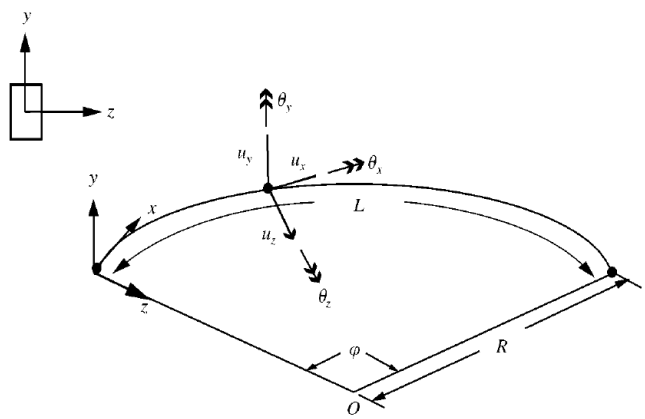

Figure 3: A general case for beam (Yang, Y. B. and Wu, C. M. (2001))

The free vibration of this system with considering the inertia of the beam can be presented by Eq. 14-17 (Yang and Wu,2001).

$$Axial\ displacement: m\ddot{u}_x + EA\left(u_x'' + \frac{u_z'}{R}\right) = 0 \tag{14}$$

$$Radial\ Displacement: m\ddot{u}_z + EI_y\left(u_z'''' + 2\frac{u_z''}{R^2} + \frac{u_z}{R^4}\right) + \frac{EA}{R}\left(u_x' + \frac{u_z}{R}\right) = 0 \tag{15}$$

$$Vertical\ displacement: m\ddot{u}_y + EI_z\left(u_y'''' - \frac{\theta_x''}{R}\right) - \frac{GJ}{R}\left(\theta_x'' + \frac{u_y''}{R}\right) = 0 \tag{16}$$

$$Torsional\ rotation: \rho J\ddot{\theta}_x + \frac{EI_z}{R}\left(u_y'' - \frac{\theta_x}{R}\right) + GJ\left(\theta_x'' + \frac{u_y''}{R}\right) = 0 \tag{17}$$

In these equations, m is mass per unit length of beam, ρ is beam density and x axis is tangent to beam. In forced vibration under moving load, force components are formed by Eq. 18-20.

$$\text{Vertical force}: f_v\delta(x - vt) \tag{18}$$

$$Horizontal\ centrifugal\ force: f_h\delta(x - vt) \tag{19}$$

$$Torque\ due\ to\ exentricity: f_v\delta(x - vt)\times d \tag{20}$$

Also, d is the load eccentricity.

f_v and f_h with considering the inertia of the load can be defined as follow (Yang et al., 2004):

$$f_v = Mg - M(\ddot{u}_y + 2v\dot{u}_y' + v^2u_y'') \tag{21}$$

$$f_h = \frac{Mv^2}{R} - M(\ddot{u}_z + 2v\dot{u}_z' + v^2u_z'') \tag{22}$$

Where M is mass of the load and v is the load velocity.

These equations have been presented in general form. Because of the high lateral inertia of bridge and independency of the vertical and lateral equations, the effect of the vehicle inertia in lateral direction is neglected.

5 SOLUTION PROCEDURE

5.1 Vertical equations

Coupled vertical and torsional equations are:

$$m\ddot{u}_y + EI_z\left(u_y'''' - \frac{\theta_x''}{R}\right) - \frac{GJ}{R}\left(\theta_x'' + \frac{u_y''}{R}\right) = f_v\delta(x - vt) \tag{23}$$

$$\rho J\ddot{\theta}_x + \frac{EI_z}{R}\left(u_y'' - \frac{\theta_x}{R}\right) + GJ\left(\theta_x'' + \frac{u_y''}{R}\right) = f_v\delta(x - vt)\times d \tag{24}$$

By using Galerkin method and consideration of sinusoidal mode shapes for each degree, the response of the beam can be considered as (Yang and Wu,2001):

$$u_k(x,t) = \sum_{i=1}^{\infty} q_{ki}(t)\sin(\frac{i\pi x}{L}) \tag{25}$$

For solving these equations, first the Eq. 23 is producted in δu_y and Eq. 24 in $\delta\vartheta_x$ and integrate them along bridge length. So equation 26 and 27 are obtained.

$$\ddot{q}_{yi} + a_1 q_{yi} + a_2 q_{\theta i} = \frac{2f_v}{mL}\sin\sin\left(\frac{\pi v t}{L}\right) \tag{26}$$

$$\ddot{q}_{\theta i} + b_1 q_{\theta i} + b_2 q_{yi} = \frac{2f_v d}{\rho J}\sin\sin\left(\frac{\pi v t}{L}\right) \tag{27}$$

Where i is the mode number and coefficients a_1, a_2, b_1 and b_2 are (Yang and Wu, 2001):

$$\begin{aligned} &a_1 = -\frac{1}{\rho J}\left[\frac{EI_z}{R^2} + GJ\left(\frac{\pi}{L}\right)^2\right], \quad a_2 = -\frac{1}{\rho J}\frac{1}{R}\left(\frac{\pi}{L}\right)^2 (EI_z + GJ), \\ &b_1 \sim \frac{1}{m}\left(\frac{\pi}{L}\right)^2\left[EI_z\left(\frac{\pi}{L}\right)^2 + \frac{GJ}{R^2}\right], \quad b_2 = \frac{1}{mR}\left(\frac{\pi}{L}\right)^2 (EI_z + GJ) \end{aligned} \tag{28}$$

By rewriting the equations 26 and 27 in matrix form, they can be solved numerically. If there is more than one load, all loads add together on the right side of the equations.

5.2 horizontal equations

Coupled radial (lateral) and longitudinal equations are:

$$m\ddot{u}_x + EA\left(u_x'' + \frac{u_z'}{R}\right) = 0 \tag{29}$$

$$m\ddot{u}_z + EI_y\left(u_z'''' + 2\frac{u_z''}{R^2} + \frac{u_z}{R^4}\right) + \frac{EA}{R}\left(u_x' + \frac{u_z}{R}\right) = f_h\delta(x - vt) \tag{30}$$

By using Galerkin method and consideration of sinusoidal mode shapes for each degree, the response of the beam can be similarly considered as:

$$\ddot{q}_{xi} + a_1 q_{xi} + a_2 q_{zi} = 0 \tag{31}$$

$$\ddot{q}_{zi} + b_1 q_{zi} + b_2 q_{xi} = \frac{2f_h}{mL}\sin\sin\left(\frac{\pi v t}{L}\right) \tag{32}$$

Where i is the mode number and also coefficients a_1, a_2, b_1 and b_2 are (Yang and Wu, 2001):

$$a_1 = \frac{\frac{EA\pi^2}{L}\left(\frac{4}{\pi^2} - \frac{1}{2}\right)}{mL\left(\frac{8}{\pi^2} - \frac{5}{6}\right)}, \quad a_2 = \frac{\frac{EA\pi}{L}\left(\frac{4}{\pi^2} - \frac{1}{2}\right)}{mL\left(\frac{8}{\pi^2} - \frac{5}{6}\right)}, \tag{33}$$

$$b_1 = \frac{EI_z}{m}\left[\left(\frac{\pi}{L}\right)^2 - \frac{1}{R^2}\right]^2 + \frac{EA}{mR^2}, \quad b_2 = \frac{EA}{mRL}\left(\pi - \frac{8}{\pi}\right)$$

By rewriting the equations 31 and 32 in matrix form, they can be solved numerically. If there is more than one load, all loads add together on the right side of the equations.

6 MODELING OF THE TRACK IRREGULARITIES

Because of the random nature of the irregularities, PSD (power spectral density) function is used to describe the irregularities. FRA has classified the irregularities of track from grade 1 to 6. Equations 34 and 35 are the PSD functions for cross and gauge irregularities ($S_{c,g}$) and elevation and alignment irregularities($S_{e,a}$) that are presented by FRA (Frýba, 1996;Wiriyachai et al., 1982).

$$S_g(\Omega) = \frac{A\Omega_2^2}{(\Omega^2 + \Omega_1^2)(\Omega^2 + \Omega_2^2)} \tag{34}$$

$$S_e(\Omega) = \frac{A\Omega_2^2(\Omega^2 + \Omega_1^2)}{\Omega^4(\Omega^2 + \Omega_2^2)} \tag{35}$$

Where Ω is the wave length of the irregularities and A, Ω_1 and Ω_2 are constants according to grade of rail that presented in table 1.

For calculating the track irregularities, Au method have been used (Au et al., 2002). In this method the irregularity can be obtained by eq. 36.

$$r(x) = \sum_{k=1}^{N} a_k \cos(\omega_k x + \varphi_k) \tag{36}$$

Where a_k is amplitude, ω_k is frequency and φ_k is a random value with a normal distribution that is in range of $(0,2\pi)$. Also, x is the location on the track and N is the number of frequency division. The terms of a_k and ω_k can be calculated as following:

$$a_k = 2\sqrt{S(\omega_k)\Delta\omega} \quad k = 1,2,\ldots,N \tag{37}$$

$$\omega_k = \omega_1 + \left(k - \frac{1}{2}\right)\Delta\omega \quad k = 1,2,\ldots,N \tag{38}$$

$$\Delta\omega = (\omega_2 - \omega_1)/N \tag{39}$$

Irregularity	Parameter		Trackclass
	Notation	Unit	3
Elevation	A	10^8 m^3	4.92
	Ω_1	10^3 m^{-1}	23.3
	Ω_2	10^3 m^{-1}	13.1
Gauge	A	10^8 m^3	3.15
	Ω_1	10^3 m^{-1}	29.2
	Ω_2	10^3 m^{-1}	23.3

Table 1: characteristic of geometry position of rails of FRA

7 SENSITIVITY ANALYSIS OF DYNAMIC RESPONSE OF BRIDGE-TRACK-TRAIN BASED ON SPEED, TRACK CURVATURE AND IRREGULARITY

The track consists of three parts: 1. 100 meters tangent section 2. 150 meters spiral section and 3. 500 meters curved section. Train enters to first and second parts and it is excited by transient oscillations, after that in steady part (curved section), the vehicle vibration approaches to steadier behavior due to track geometry. The bridge is located at middle of curved section while the steadier vibrating train is countered to bridge. This geometry causes accurate and continues changes for train-track-bridge system and avoids transients effects on bridge responses (on which depends on initial conditions). The figure 4 illustrates track geometry and bridge location.

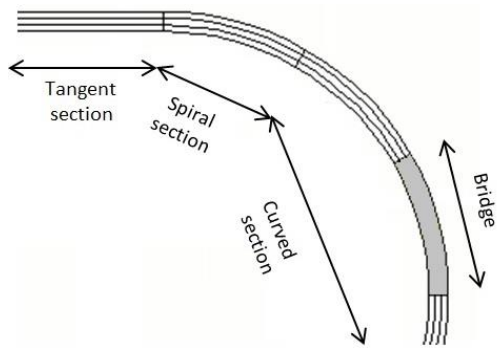

Figure 4: geometry of track and location of bridge

The considered vehicle passes over the bridge with three different velocities: 10, 15 and 20 m/s. The desired parameters that have been studied are track curvature, track irregularity and bridge span and their variation effects on bridge mid span deflections and accelerations.

Initially with a 25m span for the bridge, the effects of track curvature on vertical and lateral bridge mid span deflection have been studied. The results are shown in Fig. 5. As the radius of track curve increased, mid span vertical deflection has been decreased but lateral deflection shows an increase. In other word with increasing in track radius of curvature, the bridge tends to show a straight bridge behavior.

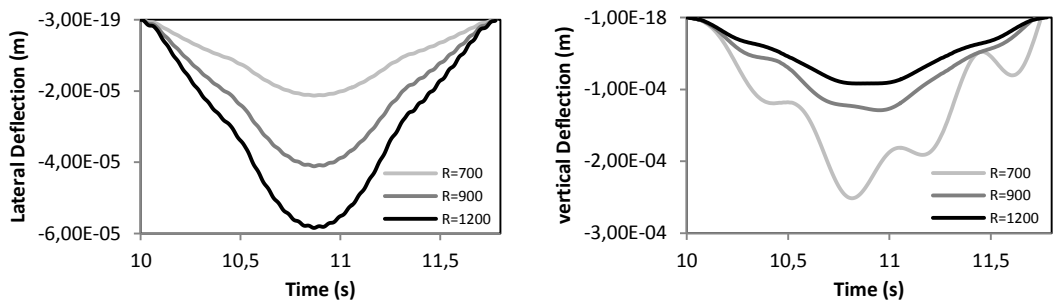

Figure 5: The effect of track curvature on bridge mid span deflection. (v=20 m/s) a) vertical deflection (right) b) lateral deflection (left)

Fig. 6 shows the vertical deflection that is independent from track irregularity and remains nearly constant. However, influence of irregularity is visible in lateral response and existence of irregularity has a maximum 40% increase in lateral response.

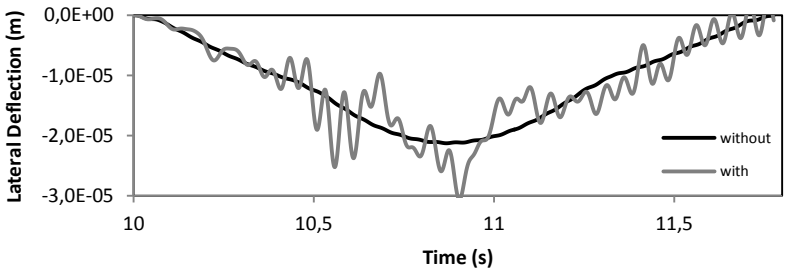

Figure 6: The effect of track irregularity on lateral response of bridge (v=20 m/s)

It should be noted that the inertia of the vehicle has overcome to effect of velocity. In moving load cases with increasing in speed of vehicle, bridge will show more deflection but due to the small bridge span length and the low weight of bridge in comparison to passing load, the effects of vehicle inertia can't be neglected. In such these cases the amount of load in each step is a function of bridge response. This phenomenon is shown in laboratory condition by Shadfar (2010). He used a 3 Kg beam with the 2m radius of curvature. Fig. 7-a shows the results for a 882 g load which pass over the beam with the speed of 1.0087 and 1.2583 m/s. Fig. 7-b also shows the results for a 263 g load which pass over the beam with the speed of 1.2028 and 1.4591 m/s.

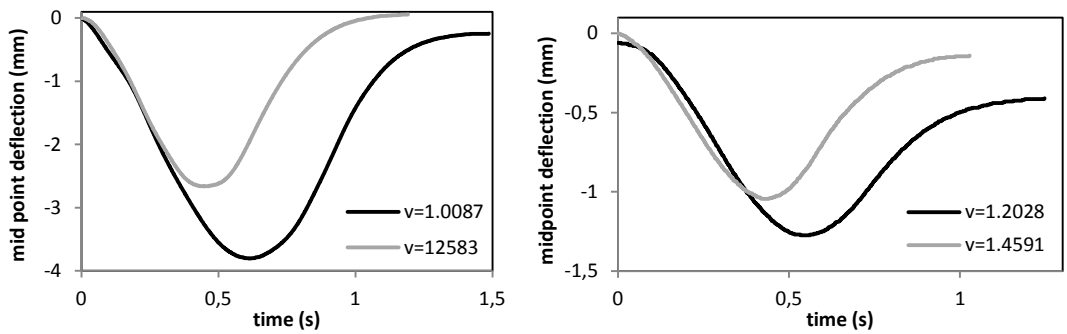

Figure 7: variations of the vertical deflection for mid-point of span in terms of various speed a) 882g load (left) b) 263g load (right)

Fig. 8 shows the effects speed on the bridge response.

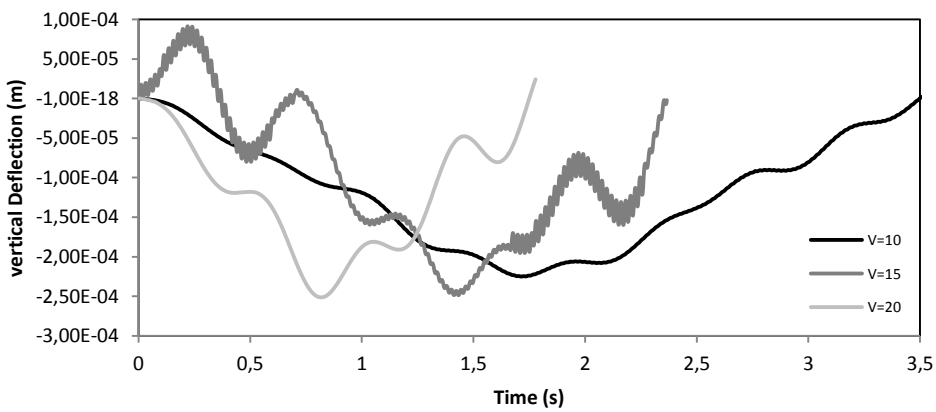

Figure 8: The effect of velocity on bridge mid span vertical deflection

In order to sensitivity analysis of the bridge, different span has been selected for the bridge and dynamical analysis was performed for each span. The span has changed from 15-25m. The results show that the bridge-track-train system is sensitive to described parameters. In Fig. 9 the results for the 20 m/s velocity are shown. With the increase in bridge span, the mass per length and moment of inertia for the bridge will be increased but the results show the lateral bridge deflection is increased and then remain constant. In vertical deflection with the increase in bridge span, deflection will be increased greatly that are shown in Fig. 9.

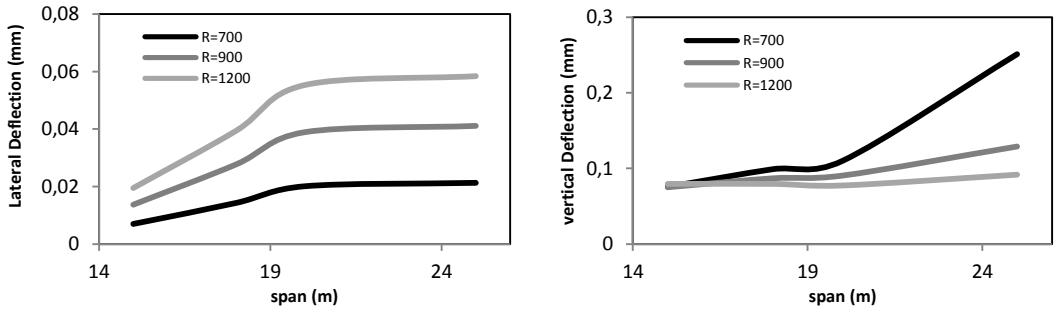

Figure 9: Changes in bridge deflection for different radius of curvature a) vertical deflection (right) b) lateral deflection (left)

For the acceleration, there are reverse pattern in results. Radius of curvature has a weak effect on vertical results but in lateral acceleration, it has a big difference in shorter spans. Besides that bridge span is principal parameters in both results that are plotted in Fig. 10.

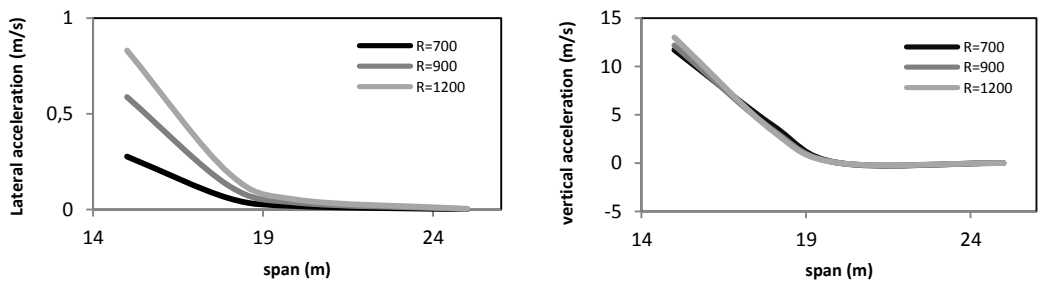

Figure 10: Effects of track radius of curvature on bridge mid span accelerations a) vertical acceleration (right) b) lateral acceleration (left)

For the irregularities as mentioned for 25m span, irregularities has a weak effect on the vertical deflection and acceleration and bridge span is the only effective on parameters in vertical direction (fig. 11), But for lateral results, there is a shift in results. So for the lateral response there is two parameters: bridge span and track quality (Fig. 12).

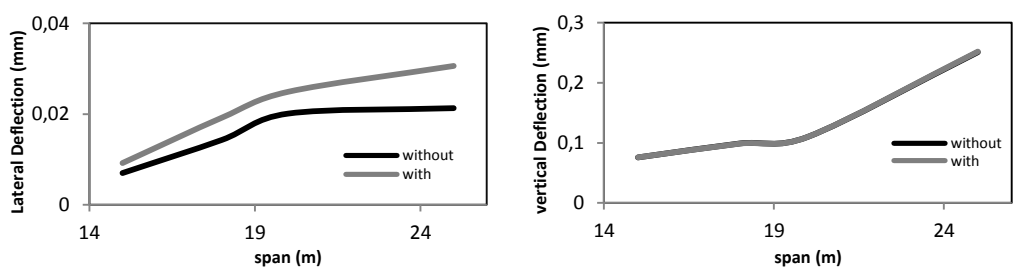

Figure 11: The effects of track irregularity on bridge deflections (track grade 3) a) vertical deflection (right) b) lateral deflection (left)

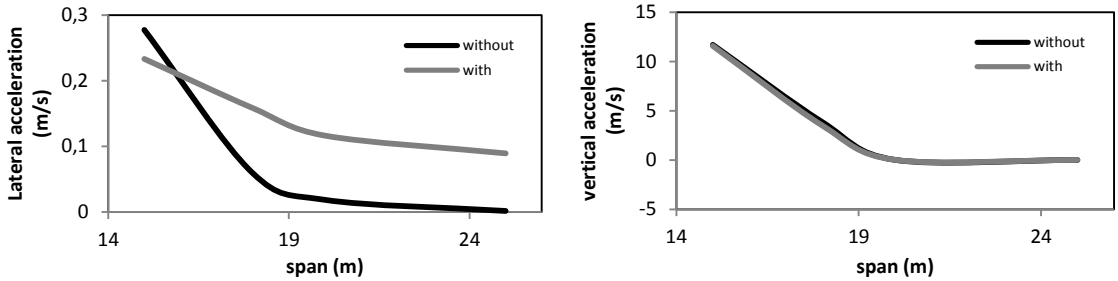

Figure 12: The effects of track irregularity on bridge accelerations (track grade 3) a) vertical acceleration (right) b) lateral acceleration (left)

For variations of speed and also with considering the vehicle inertia and increase of speed, the Disorders exist in the results especially in accelerations (Fig. 13 and 14). The total pattern shows the dominant factors of sensitivity Analysis for bridge structure are speed and bridge span in lateral results. But, in the vertical deflection, the sensitivity is not noticeable.

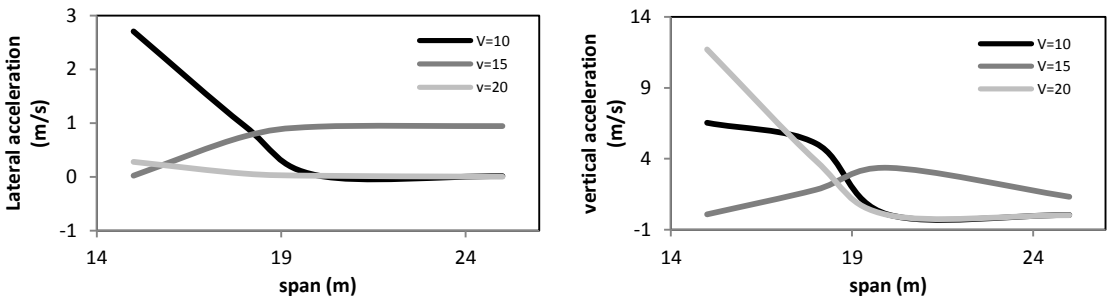

Figure 13: The effects of velocity on bridge accelerations a) vertical acceleration (right) b) lateral acceleration (left)

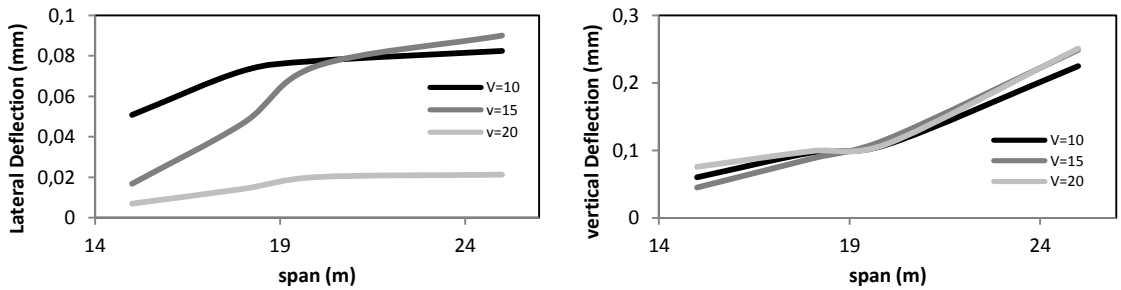

Figure 14: The effects of velocity on bridge deflections a) vertical deflection (right) b) lateral deflection (left)

8 CONCLUSION

In this study, the effects of passing vehicle over a short span bridge and the sensitivity of the structure for the dynamical parameters have been investigated by considering suspended mass on curved bridge as it has not been studied before. The results show that the bridge span, speed, track curvature, irregularities and vehicle inertia have a great influence on the bridge vertical and lateral deflection and accelerations, but in this study the effects of lateral inertia of vehicle and static deflection of the bridge are neglected. The results have been summarized as following:

1. Bridge span has an effect on vertical deflection and with increasing in the bridge span, the vertical deflection will increase, but lateral deflection increased in short spans and then remains constant. In this case study the lateral displacement remains constant from span length of 19.5m. For the accelerations with increasing in span the maximum accelerations reduced besides that the amplitudes of maximum accelerations tends to each other.
2. Track radius of curvature has a reverse effect on bridge vertical deflection and no effect on bridge vertical acceleration, but it changes in the lateral deflection and acceleration pattern.
3. In this study, irregularities have no effect on bridge vertical response but in lateral deflection it increases about 43%.
4. The effect of speed increase in vertical deflection has two separate patterns. In span of 19.5m, there is a change in patterns. Before span of 19.5m, the effect of speed has overcome to inertia whereas after one, the effect of inertia has overcome to speed. The reason of this issue is that inertia needs time to show its effect. So in larger span it has more time. In lateral deflection with an increase in speed, the maximum deflection is reduced.
5. As important new finding of this task, for short span bridge with increasing velocity the inertia effect reduced while the gravity effect increased, this pattern is different routine solution of long span bridge exited by moving loads. So for short span bridge the effect of inertia should be considered for accurate results.

9 SYMBOLS

m_w	Wheelsetmass	1300kg	m_t	Bogieframemass	2200kg
r_0	Wheelradius	0.42m	a	Halfoftrack gauge	0.7175m
λ	Wheelconicity	0:05	d	Flangeclearance	0.00923m
f_{11}	Lateral creepforcecoefficient	2.212e6N	f_{12}	Lateral/spincreepforcecoefficient	3120Nm^2
f_{22}	Spincreepforcecoefficient	16N	f_{33}	Longitudinalcreepforcecoefficient	2.563e6N
μ	Coefficientoffriction	0.2	m_c	Carbodymass	3.1e4kg
K_{px}	Longitudinalstiffnessofprimarysuspensión	1.4e6N/m	K_{py}	Lateral stiffnessofprimarysuspension	1.4e6N/m
K_{pz}	Verticalstiffnessofprimarysuspensión	1e6 N/m	C_{pz}	Verticaldampingofprimarysuspension	526737Ns/m
K_{sx}	Longitudinalstiffnessofsidebearings	1e5 N/m	K_{sy}	Lateral stiffnessofsidebearings	1e5 N/m
K_{sz}	Verticalstiffnessofsidebearings	5.7e5 N/m	C_{sx}	Longitudinaldampingofsidebearings	0 N.s/m
C_{sy}	Lateral dampingofsidebearings	0 N.s/m	C_{sz}	Verticaldampingofsidebearings	1000 N.s/m
b_1	Halfofprimarylongitudinal and verticalspring / dampingarm	1.0 m	b_2	Halfofsecondarylongitudinal and verticalspringarm	1.18m
b_3	Halfofsidebearingslongitudinal and verticaldampingarm	1.4 m	N	Normalforceactingonwheelsetinequilibriumstate	225000 N
L_2	Halfofprimarylateral dampingarm	1.5 m	L_1	Halfofprimarylateral springarm	1.28m
L_c	Longitudinaldistancefromwheelsetcenterofgravitytocarbody	4.2 m	h_T	Verticaldistancefromwheelsetcenterofgravitytosidebearings	0.47m
I_{wx}	Rollmomentofinertiaofwheelset	688kg.m^2	I_{wy}	Spinmomentofinertiaofwheelset	100kg.m^2
I_{wz}	Yawmomentofinertiaofwheelset	688kg.m^2	I_{tx}	Rollmoment ofinertia ofbogieframe	1995kg.m^2
I_{tz}	Yawmomentofinertiaofbogieframe	2850kg.m^2	I_{cx}	rollmoment ofinertia ofcarbody	3.7e4kgm^2
I_{cz}	yawmoment ofinertia ofcarbody	2.98e4kgm^2	A	bridge crossectionarea	3.5~10.5 m^2
L	bridge span	15-25 m	ρ	bridge density	2400 Kg/m^2
I_y	bridge vertical moment of inertia	12.2424~ 73.4544 m^4	I_z	bridge lateral moment of inertia	0.7228~ 4.3368 m^4

References

Au, F. T. K., Wang, J. J., Cheung, Y. K. (2002). Impact study of cable-stayed railway bridges with random rail irregularities, Engineering Structures, Volume 24, Issue 5, pp. 529–541

Cheng, Y. C., Lee, S. Y., Chen, H. H. (2009). Modelling and nonlinear hunting stability analysis of high-speed railway vehicle moving on curved tracks, Journal of Sound and Vibration 324, pp. 139–160

Esmailzadeh, E., Jalili, N. (2003). Vehicle–passenger–structure interaction of uniform bridges traversed by moving vehicles, Journal of Sound and Vibration 260, pp. 611–635

Frýba, L. (1996). Dynamics of Railways Bridges, Thomas Telford House, Czech Republic

Fryba, L. (1972). Vibration of solids and structures under moving loads, Thomas Telford, Czech Republic, ISBN 0-7277-2741-9

Fryba, L. (1976). Non-stationary response of a beam to a moving random force, Journal of Sound and Vibration, 46, (3), pp. 323-338

Fryba, L. (1980). Estimation of fatigue life of railway bridges under traffic loads, Journal of Sound and Vibration, 70, (3), pp. 527-541

Frýba, L. (1996). Dynamics of Railways Bridges, Thomas Telford House, Czech Republic

Ghazi Zadeh, A. (2010). Analysis of torsional and lateral coupled vibration of beams under moving eccentric loading, BSc. Thesis (in Persian), Iran University Science and technology, Iran

Iwnicki, S. (2003). Simulation of wheel-rail contact forces, Fatigue & Fracture of Engineering Materials & Structures, Volume 26, Issue 10, pp. 887–900, October 2003

Shadfar, M. (2010). Analysis of torsional and lateral coupled vibration of curved bridge under moving eccentric mass, BSc. Thesis (In Persian), Iran University Science and technology, Iran

Song, M. K., Noh, H. C., Choi, C. K. (2003). A new three-dimensional finite element analysis model of high-speed train–bridge interactions, Engineering Structures 25, pp. 1611–1626.

Wiriyachai, A., Chu, K. H., Garg, V. K. (1982). Bridge impact due to wheel and track irregularities, Journal of the Engineering Mechanics Division, Vol. 108, No. 4, pp. 648-666

Xia H., Xu Y. L., Chan T. H. T. and Zakeri J. A (2007). Dynamic Responses of Railway Suspension Bridges under Moving Train, Scientia Iranica Vol. 14, No. 5, 385-394.

Yang, Y. B., Wu, C. M. (2001). Dynamic response of a horizontally curved beam subjected to vertical and horizontal moving loads, Journal of Sound and Vibration 242(3), pp. 519-537

Yang, Y. B., Yau, J. D., Wu, Y. S. (2004). Vehicle-Bridge Interaction Dynamics: With Applications To High-Speed Railways, World Scientific Publishing Co. Pte. Ltd., 5 Toh Tuck Link, Singapore 596224

Yau, J.D. (2009). Response of a train moving on multi-span railway bridges undergoing ground settlement, Engineering Structures 31, 2115_2122.

Zacher, M. Dynamics of a Train over a Flexible Bridge, 15th European ADAMS Users' Conference

APPENDIX

By considering axis x,y and z for longitudinal, lateral and vertical direction, φ for roll (rotation about x axis), χ for pitch (rotation about y axis) and ψ for yaw rotation (rotation about z axis) creepages could be calculated with the help of equations:

$$\xi_{lx} = 1 - \frac{r_l \dot{\chi}}{V} + \frac{\dot{x} - a_l \dot{\psi}}{V}, \qquad \xi_{rx} = 1 - \frac{r_r \dot{\chi}}{V} + \frac{\dot{x} + a_r \dot{\psi}}{V}$$

$$\xi_{ly} = \left(-\psi + \frac{\dot{y} + r_l \dot{\varphi}}{V}\right)\cos\delta_l + \frac{\dot{z} + a_l \dot{\varphi}}{V}\sin\delta_l, \qquad \xi_{ry} = \left(-\psi + \frac{\dot{y} + r_r \dot{\varphi}}{V}\right)\cos\delta_r + \frac{\dot{z} - a_r \dot{\varphi}}{V}\sin\delta_r$$

$$\xi_{ls} = \frac{-\dot{\chi}\sin\delta_l + \dot{\psi}\cos\delta_l}{V}, \qquad \xi_{rs} = \frac{-\dot{\chi}\sin\delta_r + \dot{\psi}\cos\delta_r}{V}$$

Where δ represent instantaneous wheel conicity. Indices l and r are for left and right wheels. With the help of linear theory of Kalker, contact forces between wheel and rail as a contact element, could be calculated as follows:

$$F_x = f_{11}\xi_x$$
$$F_y = f_{22}\xi_y + f_{23}\xi_{sp}$$
$$M_z = f_{23}\xi_y + f_{33}\xi_{sp}$$
$$where: \begin{cases} f_{11} = (\frac{N}{N_0})^{(2/3)} f_{110}, \quad f_{23} = (\frac{N}{N_0}) f_{230} \\ f_{22} = \left(\frac{N}{N_0}\right)^{\frac{2}{3}} f_{220}, \quad f_{33} = \left(\frac{N}{N_0}\right)^{\frac{4}{3}} f_{330} \end{cases}$$

f_{ij0} are Kalker creep coefficients, N is instantaneous vertical load and N_0 is static wheel load.